

Application of Laser Interferometry in Detecting Deformation of the Cherenkov Telescope

Yiran Yin,^{a,*} Long Chen,^{a,*} Fengrong Zhu,^a Yang Wang^a and Min Jin^a

^a*School of Physical Science and Technology, Southwest Jiaotong University Chengdu, 611756, Sichuan Province, China*

E-mail: longchen@swjtu.edu.cn

The Cherenkov Telescope was designed to study high-energy cosmic ray. The Large Telescopes and Medium Telescopes in the Cherenkov Telescope Array are usually equipped with photomultiplier tubes(PMT) or silicon photomultipliers(SiPM). These detectors are used to detect the Cherenkov light produced by the interaction of gamma rays with the atmosphere. The mirror system and the PMT(SiPM) are supported from each other by rigid supports, their relative position is critical to ensure high angular resolution. Laser interferometric methods are used to measure changes in the position of the PMT detector, which may be affected by gravity, temperature, wind, or other factors, and can also be used to detect the deformation of the telescope mirror. More accurate data can be obtained by nanoscale displacement in real time . This paper focuses on laser interferometry remote measurement of nanoscale displacements and high-precision displacement signal processing. The present study establishes a laser interferometry system and collects interference signals, which indicate distance consistency and validate the feasibility of the system.

38th International Cosmic Ray Conference (ICRC2023)
26 July - 3 August, 2023
Nagoya, Japan



*Speaker

1. Introduction

The large telescope mainly uses the high-precision astronomical positioning and high-precision tracking system to measure and track the target, which consists of two main parts: the receiving system and the antenna. The most common type of antenna used in large telescopes is the reflector antenna, which is composed of a patchwork of small sub-mirrors[1]. The reflection accuracy, shaking accuracy, friction torque and other parameters of large telescopes will have a great impact on the pointing accuracy of the reflector surface of the telescope[2]. With the development of modern science and technology, the manufacturing technology of the antenna has been significantly improved, and the aperture size of the reflector antenna has gradually increased from 10m to 30m-100m [3, 4]. The influence of gravity and temperature gradient on the deformation of the reflector increases significantly, and the total square mean root error of the reflector accuracy increases. It is necessary to detect and adjust the reflector to keep its parabolic shape[5]. Therefore, in the process of optimization of large telescopes, the research of reflection surface detection technology of large telescopes has been paid much attention.

The laser tracker is the key device of the inspection telescope reflection system, it plays the role of measuring the reflecting surface and determining the deviation from the theoretical reflecting surface. The system laser tracking measurement system uses a single laser tracker as the sensor and the measurement principle of polar coordinates for fast tracking measurement coordinate repeat measurement[6]. By moving the reflecting device over the surface of the object to be measured, the surface can be digitized quickly. Foreign laser trackers are used to align the main reflector panel and verify the square root mean error of the panel after installation[7]. The laser tracking system needs further optimization because the distance between the tracking head and the measurement target is too large and the measurement data is susceptible to air turbulence errors along the tracker beam path[8].

In this present, two mirrors are used in the optical path to collimate the laser beam in the independently designed system. In the circuit, the effect of noise is effectively reduced by directly connecting the appropriate resistance to the photoelectric conversion circuit. A new scheme was proposed to calibrate the position change of PMT detector. By setting four target points on PMT, laser interferometry measured the relative position change of the four target points, and improved the measurement accuracy of Large telescope after calibration. At the same time, the method of laser interferometry can be used to calibrate the mirror of the telescope.

2. Principle scheme

2.1 Development of Framework

The traditional laser interference system is mainly divided into two types from the principle of single-frequency laser interference system and dual-frequency laser interference system, both systems are composed of laser system, interference system, signal processing system three parts, the following is a brief introduction to the basic principles of the two types, mainly for its opticalpath part. The laser light source of the conventional single-frequency laser interference system uses

a single-frequency laser, and its optical path structure is similar to the Michelson interferometer structure. The layout shown as Figure 1.

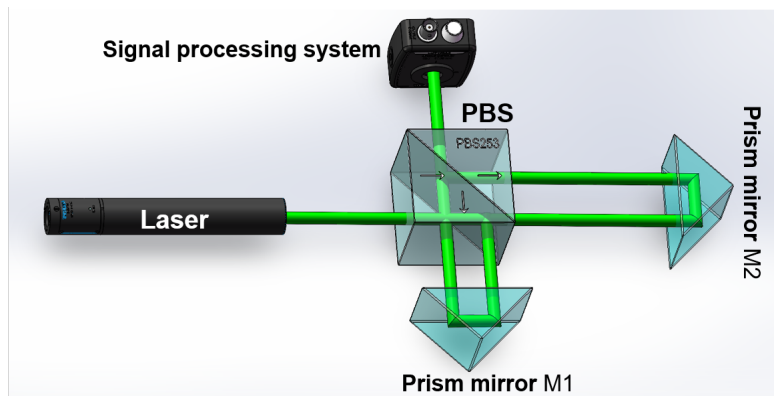


Figure 1: Schematic diagram of single frequency laser interference

Splitter P divides the light source beam from the single-frequency laser into two parts. One beam of reflected light is reflected by the fixed reflector M1 and returned to the splitter P; the other beam of transmitted light is reflected by the movable reflector M2 and returned to the splitter P. When the two beams of reflected light converge at the splitter P, interference phenomenon can be generated, which is the optical path part of the interferometric measurement system. Then use the signal processing system to process the information of the interferometric beam, you can get the desired measurement data, this process needs to design the circuit for photoelectric conversion.

The device involved in single-frequency laser interferometry is relatively simple and low cost, and there is no limit to the movement of the reflector, but since the single-frequency laser interferometry is based on DC amplitude modulation signal processing, it is susceptible to the interference of external ambient light, which leads to counting errors. Dual-frequency laser interferometry has the advantages of small signal affected by DC drift and strong anti-interference ability, but due to its limited measurement speed and large measurement non-linearity error, it is difficult to realize correction and compensation, which restricts the measurement accuracy, and generally has expensive acoustic and optical frequency shift devices, and the optical path structure is more complex. This thesis is a preliminary work, and a relatively simple structure of single-frequency laser is chosen to build the interference system.

2.2 Practical scheme

The PMT camera is an important part of the large telescope. The PMT camera is installed on the top of the large telescope mirror system by supports. When large telescope points at different elevation angles, gravity deformation will occur due to the influence of gravity, and other factors will cause deformation, such as the deformation caused by wind, with high frequency and irregularity. It is necessary to calibrate PMT because the small displacement caused by various deformations can cause errors in the measurement data. The specific scheme is as follows: install four target points at the four corners of the PMT camera, and the four target points are monitored by four optical paths derived from the laser interferometer, and the linear displacement, angular displacement and

vertical displacement of the PMT camera are respectively measured. The layout shown as Figure 4(a) and 4(b).

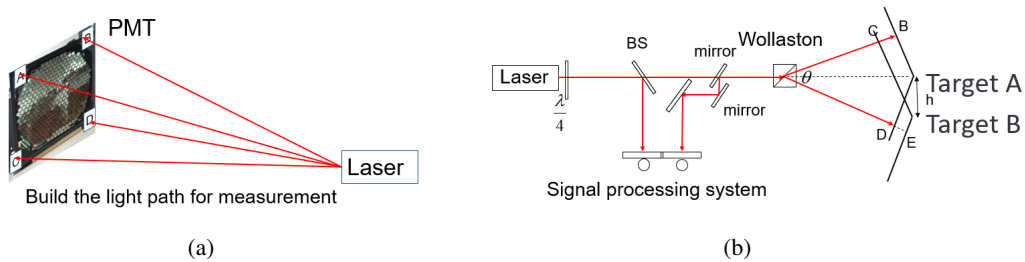


Figure 2: (a):Schematic design of laser calibration PMT; (b):Schematic diagram of laser interferometry measurement of vertical displacement.

The large telescope has very high requirements for the pointing degree of the mirror, so the calibration of the mirror becomes inevitable. The error between the indicated position of the telescope and the actual position of the celestial body is called the pointing error. There are many reasons for the formation of the telescope pointing error, mainly atmospheric refraction, telescope manufacturing and assembly errors, gravitational deformation of the telescope structure and deformation errors caused by temperature changes or temperature gradients. These errors have the characteristics of repeatability, and some factors have the characteristics of random changes, so these can not be corrected, mainly the empty return in the kinematic chain, the gap and the hysteresis effect in the structure.

If all the linear correlation in the various error laws are obtained as a function of expression, then the total pointing error is the sum of all these functions, for the telescope mirror calibration can be used as follows: thermal gradient deformation (tabulation), thermal expansion and contraction semi-closed-loop correction control system based on temperature measurement and finite element model, gravity deformation (tabulation): pointing to different elevation angles, open-loop correction control system with finite element model, other deformations: wind causes deformation , high frequency, closed-loop control system based on large scale surface shape measurement technology.

3. Laser interference experiment

3.1 Optical path design

The system designed in this paper is built on the basis of Michelson-type interferometric system, in which the optical path and circuit parts are shown in the following figure. For the optical path, a 5-fold beam expander is selected to expand the beam from the laser, while two plane mirrors are selected to adjust the angle of the plane mirror to solve the problem of beam misalignment. The collimated light beam enters the spectroscop P and is divided into two parts. One of the reflected light beams is reflected back to the spectroscop through the fixed mirror M1, and the other transmitted light is reflected back to the spectroscop through the reflection of the movable mirror, and the two beams are merged here. Since the maximum detection signal that can be detected by the photodetector is 10mW, and the output power of the laser is 55mW, in order to

prevent the damage of the photodetector, the laser energy will be attenuated by adding a damping plate in front of the photodetector. The specific parameters of the laser are shown in the following table 1. For the circuit part of the measurement system, after the optical path part can produce stable interference fringes, the interference beam is connected to the photodetector to convert the optical signal into the current signal. After converting the current signal to voltage signal by trying different solutions such as current-voltage converter and voltage regulator, we choose to connect the current obtained from the photodetector directly to the two ends of the resistor and then connect the voltage value of the two ends of the resistor to the computer. The layout shown as Figure ??.

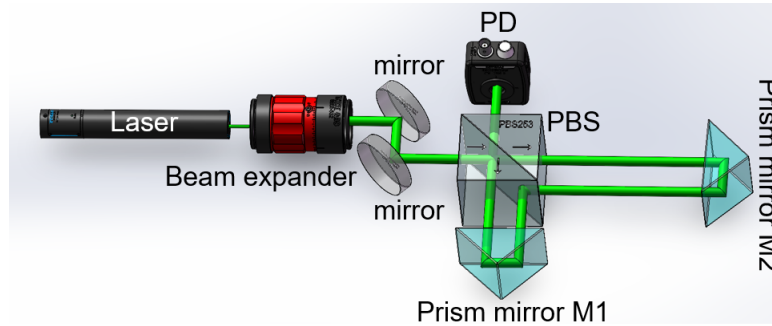


Figure 3: Design diagram of light path

Install the AD acquisition card into the mainframe of the laboratory computer, and connect the current detected by the photodetector to the two ends of the three-thousand ohm resistor, then use the wire to connect the voltage at the two ends of the resistor to the acquisition card, and open the data acquisition interface. After the successful data acquisition, for the processing of the collected signal waveform, starting from the initial recording, for every half wavelength distance moved by the moveable reflector, the optical range difference changes by one wavelength, the interference fringe in the field of view moves by one, and the acquisition card also collects a complete waveform. By counting the number of waveforms in the acquisition process, it can be deduced that the moving distance of the movable reflector ΔL can be expressed as:

$$\Delta L = \lambda/2(N + \xi) \quad (1)$$

λ denotes the laser wavelength for that environment, and N represents the number of complete waveforms recorded by the acquisition card, indicating the proportion of incomplete waveforms. Since the moveable reflector cannot move at a distance that corresponds to an integer multiple of exactly half a wavelength, the handling of incomplete waveforms is very important.

3.2 Laser interference data processing

Due to the existence of environmental disturbances and laser instability, in order to minimize the influence of external uncontrollable factors on the measurement results, the experimental site was quiet and the lights were turned off for measurement. After turning on the laser light source for ten minutes to warm up, the voltage values were recorded when there was interference information into the photodetector. For the case without light source, the minimum and maximum values of voltage are -0.0061 V and 0.0067 V respectively, with a difference of 0.0128 V, which is a good

Table 1: laser parameters

Item	Unit	Measurement result
Central emission wavelength	nm	532.3
Nominal output adjustment	mw	50
Power stability over 8 overs	pk-pk	0.19
Beam waist diameter at 1/e ² ,5cm from output aperture	mm	0.69

noise suppression effect compared with the case of using current-voltage converter and regulated power supply. For the stable interference fringe, the minimum and maximum values of voltage are 0.7081 V and 0.7404 V, respectively, with a difference of 0.0323 V. It can be seen that the fluctuation range is larger when there is light into the detector, and it is guessed that the laser source is not stable enough. Measure the change in voltage value with slight rotation of the movable reflector. It can be calculated that the average value of the initial more stable voltage is approximately 0.68525 V, and the average value of the final more stable voltage is approximately 0.70307 V. The layout shown as Figure 4(a).

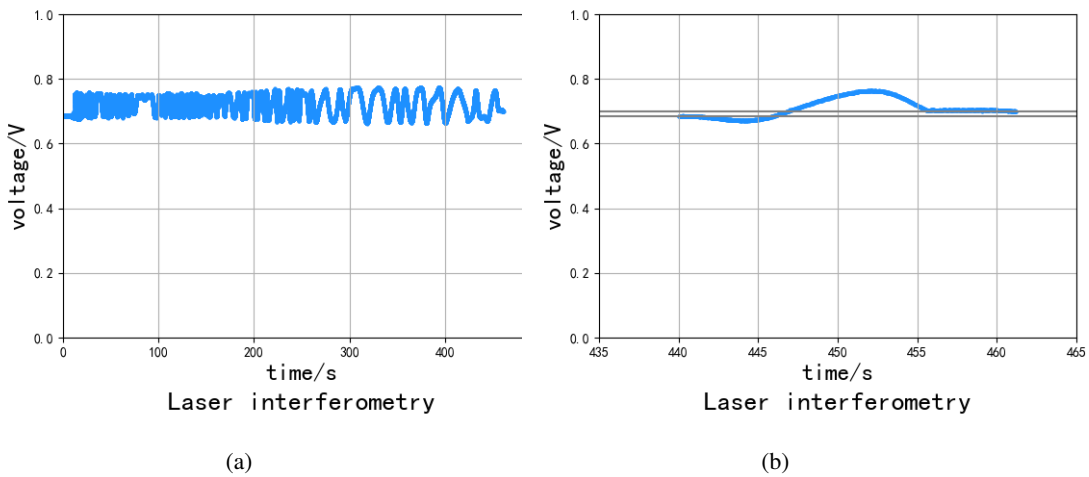


Figure 4: (a):Diagram of laser interferometry data processing; (b):Laser interferometry end data processing diagram;

For the period number of the waveform, the complete waveform can be counted by plotting it in sections, and then the individual waveforms at the end with incomplete periods can be analyzed. The specific situation is shown in the figure below. The waveforms vary in size due to the speed at which the micrometer filament of the moveable mirror is turned, but a complete waveform is one that has moved a half wavelength. There are 54 complete waveforms in total. The following is the method for dealing with a waveform with a non-complete period at the far end:

- a. Find out the minimum and maximum value of the waveform;

b. Simplify the 1/2 waveform in accordance with the trigonometric function. This example sets the minimum voltage at the origin and the maximum voltage at point C in the waveform segment.

c. Dealing with the voltage values of the initial and end states, point A indicates the initial voltage measurement, and point B indicates the voltage measurement at the end, both of which are the average value of a period of stability time.

d. According to the incomplete waveform, the proportion of the non-integer period in the period can be obtained as 0.7726 by programming. The layout shown as Figure 4(b). Experiments show that the refractive index of the air changes by 1.47×10^{-10} when the concentration of carbon dioxide in the air increases by 1ppm.

Number of complete period $N=54$, non-complete period $\xi=0.7726$. The air condition can be calculated, that is, under the conditions of temperature $t=15.5\text{ }^{\circ}\text{C}$, pressure $P=101600\text{ Pa}$, humidity $f=43\%$ and carbon dioxide content $x=550\text{ ppm}$, the refractive index n is 1.00027848.

According to the laser wavelength of 532.3 nm under vacuum and the relationship between the laser wavelength in air and the laser wavelength in vacuum equation:

It can be calculated that the laser wavelength in this air is 532.1518 nm, and it can be seen that $\Delta L = \lambda/2(N + \xi)$ where λ represents the laser wavelength of the environment, N represents the number of complete waveforms recorded by the acquisition card, and ξ represents the proportion of non-complete waveforms. It can be calculated that the moving distance of the movable mirror is 14537.669 nm, that is, 14.537669 μm , which is basically consistent with the manual fine-tuning of the micrometer filament of 0.014 mm. The voltage value without laser into the photodetector and with laser into the photodetector and the movable reflector stationary within 15 seconds was tested on the successfully built single frequency laser interferometry system to verify the stability and noise removal of the experiment. Finally, the stability of the experimental system was verified by slightly rotating the micrometer filament of the movable mirror by hand, and comparing the experimental data by analyzing the number of interference fringe changes, which verified that the currently designed photoelectric conversion circuit greatly reduces the influence of external noise and has good stability. At the same time, it is also found that the laser light source is not mentioned stable, which provides the basis for the subsequent improvement of the stability of the laser light source. In addition, the measured data of the small displacement were processed by the method of waveform subdivision, and the measured value was basically in line with the actual value to verify the accuracy of the experiment.

4. Summary

The laser interferometry method has incomparable advantages in measuring micro-displacement. In this paper, we propose a new scheme to measure micro-displacement of PMT(SiPM) by laser interferometry, and design and set up a set of single-frequency laser interferometry system. By designing the photoelectric conversion part and conducting stability experiments, the influence of external noise is effectively reduced. In addition, we conducted the microdisplacement measurement experiment, analyzed and processed the interference fringe information by waveform subdivision, calculated the microdisplacement value and compared it with the displacement of rotation of the micrometer filament rod on the base of the movable reflector. Since the wavelength was affected by

the environment, we used the Edlen refractive index calculation formula, and added the influence factor of carbon dioxide based on the improved formula to improve the measurement accuracy.

Acknowledgements

This work was supported by National Key RD program of China (2021YFA0718403) and NSFC (12105233, 12173039).

References

- [1] Souccar K, Wallace G, Grosslein R, et al. The architecture of the active surface control system of the Large Millimeter Telescope[C]//Advances in Optical and Mechanical Technologies for Telescopes and Instrumentation. SPIE, 2014, 9151: 874-879.
- [2] Schloerb F P, Sanchez D, Narayanan G, et al. Calibration and operation of the active surface of the Large Millimeter Telescope[C]//Ground-based and Airborne Telescopes VI. SPIE, 2016, 9906: 2208-2214.
- [3] Gale D M. Experience of primary surface alignment for the LMT using a laser tracker in a non-metrology environment[C]//Ground-based and Airborne Telescopes IV. SPIE, 2012, 8444: 1649-1664.
- [4] Nikolic B, Hills R E, Richer J S. Measurement of antenna surfaces from in-and out-of-focus beam maps using astronomical sources[J]. *Astronomy Astrophysics*, 2007, 465(2): 679-683.
- [5] Nikolic B, Prestage R M, Balser D S, et al. Out-of-focus holography at the Green Bank Telescope[J]. *Astronomy Astrophysics*, 2007, 465(2): 685-693.
- [6] Leon-Huerta A, Alvarez M L, Rios E H, et al. Alignment of a large outdoor antenna surface using a laser tracker[C]//Optical Measurement Systems for Industrial Inspection VIII. SPIE, 2013, 8788: 893-900.
- [7] Burge J H, Su P, Zhao C, et al. Use of a commercial laser tracker for optical alignment[C]//Optical system alignment and tolerancing. SPIE, 2007, 6676: 132-143.
- [8] Muralikrishnan B, Phillips S, Sawyer D. Laser trackers for large-scale dimensional metrology: A review[J]. *Precision Engineering*, 2016, 44: 13-28.